CSIRO PUBLISHING

Australian Journal of Physics

Volume 50, 1997

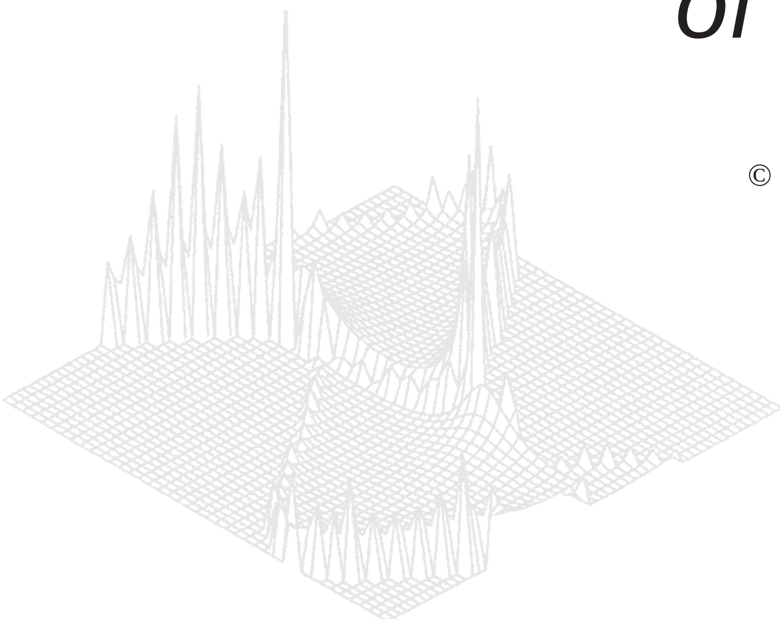

A journal for the publication of
original research in all branches of physics

www.publish.csiro.au/journals/ajp

All enquiries and manuscripts should be directed to
Australian Journal of Physics
CSIRO PUBLISHING
PO Box 1139 (150 Oxford St)
Collingwood
Vic. 3066
Australia

Telephone: 61 3 9662 7626
Facsimile: 61 3 9662 7611
Email: peter.robertson@publish.csiro.au

Published by **CSIRO** PUBLISHING
for CSIRO Australia and
the Australian Academy of Science

Aust. J. Phys., 1997, **50**, 803–13

Stimulated Vacuum Pair Production in a Focused Laser Field

P. M. Derlet, H. S. Perlman and G. J. Troup

Department of Physics, Monash University,
Clayton, Vic. 3168, Australia.

Abstract

The quantum electrodynamical process of vacuum pair production in the presence of a focused laser field is investigated. A coherent states picture of the electromagnetic field in the focal region is developed which facilitates its inclusion into perturbative S-matrix quantum electrodynamics. The lowest order differential transition rate with respect to the direction of the newly created positron is presented for a number of scattering geometries. It is found that with current technological trends such an event should be detectable in the not too distant future.

1. Introduction

Recent developments in hard X-ray laser technology may in the near future provide an environment in which the stimulated vacuum* production of electron–positron pairs becomes an observable event. In this paper we present the lowest order differential transition rate for the quantum electrodynamical process of pair creation in the focal region of a hard X-ray laser device.†

Quantum electrodynamics (QED) in the presence of a focused *optical* laser field has been investigated extensively since the inception of vacuum QED in the early fifties (Becker 1991). Typically the wavelength(s) of the non-laser particles are many orders of magnitude less than that of the laser photons. This extreme disparity between the interaction region of the non-laser particles and the near macroscopic inhomogeneities of the image space laser field allows the focal region to be approximated by a transverse plane wave of infinite extent. From a theoretical perspective such an approximation facilitates the use of the exact solution of a Dirac fermion in an external classical transverse plane wave field; the Volkov (1935) solution, in conjunction with QED in the bound interaction picture representation (Jauch and Rohlich 1980).

The theoretical predictions of fundamental processes such as stimulated bremsstrahlung and single photon pair production (Nikishov and Ritus 1967), stimulated Möller scattering (Oleinik 1967) and Compton scattering (Oleinik 1968) have met with success for a relatively modern class of experiments (McDonald

* In the present context this entails the traditional QED vacuum and the electromagnetic field.

† This work has been presented in part at ALCOLS 93, University of Melbourne, Australia, and at LXXX Congresso Nazionale, SIF, Lecce, Italy 1994.

10.1071/PH96104 0004-9506/97/040803$05.00

1992) that employ an intense pulsed optical laser system known as the table top terrawatt (T^3) laser system (Normand *et al.* 1990; Squire *et al.* 1991; Sauteret *et al.* 1991) which, when focused, can achieve power densities of up to 10^{18} W cm^{-2} for a short period of time.

The plane wave approximation is expected to no longer hold for increasing frequency and more strongly focused systems. Indeed, we have recently reported on the breakdown of the plane wave approximation for the stimulated bremsstrahlung differential and total transition rates (Derlet *et al.* 1995). Moreover, in the present context, the plane wave approximation must immediately be abandoned since the creation of a real electron and positron pair is not possible when solely in the presence of an external transverse plane wave due to the single laser photon momentum mode available. That is, the energy–momentum conservation rule in 4-vector notation is $nk = p^+ + p^-$ which reduces to $(p^+p^-) = -m^2$, a condition not satisfied by real fermions. Here k is the 4-momentum of the photon, p^+ (p^-) is the 4-momentum of the positron (electron) and n is an integer corresponding to the number of laser photons contributing to the creation process.

However, with a more realistic representation of the focused field, the associated real space variation of the electric field in the focal region would entail a broad photon momentum spectrum allowing for example, the lowest order process involving the four-momentum equation: $k_1 + k_2 = p^+ + p^-$ (where k_1 and k_2 are the four-momentum of photons from the focused laser field) to be satisfied, thus facilitating the creation of real electron–positron pairs.

To investigate the stimulated vacuum pair production process, the plane wave approximation must be replaced with a more realistic description of the focal region. Unfortunately, the Volkov solution is then no longer applicable and a necessarily perturbative approach with respect to the external laser field is needed. Throughout this work the natural system of units is used where the natural unit is chosen to be the electron volt.

Historically, the stimulated vacuum pair production rate has been investigated in the limit $\omega_{\mathrm{laser}} \ll 2m_0$, where ω_{laser} is the laser frequency and m_0, the rest mass of the electron. In this regime, the focal region can be represented by a constant electric field and an application of Schwinger's proper time method results in an analytic expression for the pair creation amplitude (Schwinger 1951; Brezin and Itzykson 1970) which is non-perturbative with respect to the laser field. In this regime, the pair creation process is a multi-laser photon process, whereas in the limit $\omega_{\mathrm{laser}} \gg 2m_0$, it is a few-laser photon process and therefore amenable to a perturbation expansion with respect to the laser field.

It is known that for a constant (and alternating) electric field in the intermediate case ($\omega_{\mathrm{laser}} \sim 2m_0$), there exists a non-trivial cross-over between the above-mentioned limits, for which neither remains valid (Caldi 1992). To date, there is however no similar detailed understanding for strongly inhomogenous external laser fields; the evaluation of the vacuum–vacuum transition rate:

$$\langle 0|S|0\rangle = \langle 0|T \exp\left[-ie\int d^4x\overline{\psi}(x)\gamma^\mu\psi(x)A_{e\mu}(x)\right]|0\rangle, \tag{1}$$

from which the stimulated vacuum–vacuum pair production rate can be derived, clearly becoming intractable.

As an initial attempt at obtaining the differential stimulated pair production transition rate for hard X-ray and strongly focused laser fields, we employ a perturbation expansion with respect to the laser field. In light of the above discussion, even though the photon number density in the focal region will be far from the intense field regime, our present calculation can realistically be regarded as only an order of magnitude estimate calculation in which we can obtain, for the first time, the angular distribution of the emerging positrons.

2. QED in a Focused Laser Field

In the present work we represent the laser field in terms of coherent states. This provides a direct and intuitive relationship between a classical electromagnetic field and the (momentum) distribution of the corresponding photon field (Glauber 1951, 1963). A generalised coherent state $|\psi\rangle$ is given by

$$|\psi\rangle = \prod_{\vec{q},r} \otimes |\rho_{\vec{q},r}\rangle \,, \tag{2}$$

where $|\rho_{\vec{q},r}\rangle$ is a coherent state satisfying the eigenvalue equation $a^{\dagger}_{\vec{q},r}|\rho_{\vec{q},r}\rangle = \rho_{\vec{q},r}|\rho_{\vec{q},r}\rangle$. Here $a^{\dagger}_{\vec{q},r}$ is the creation operator for a photon with wave vector $\vec{q}$ and spin r, and $\rho_{\vec{q},r}$ an arbitrary complex number whose magnitude squared is the eigenvalue of the photon number operator of the particular oscillation mode. More generally $|\psi\rangle$ satisfies the eigenvalue equation $A^{\mu}(x)|\psi\rangle = A^{\mu}_{e}(x)|\psi\rangle$, where $A^{\mu}(x)$ is the QED photon field operator and

$$A^{\mu}_{e}(x) = \sum_{\vec{k},r} \frac{\varepsilon^{\mu}(\vec{k},r)\rho_{\vec{k},r}}{\sqrt{2V\omega_{\vec{k}}}}[\exp(-ikx) + \exp(ikx)] \,, \tag{3}$$

in which $\varepsilon^{\mu}(\vec{k},r)$ is the photon polarisation vector associated with the wave vector $\vec{k}$ and spin r. It is the c-numbers, $A^{\mu}_{e}(x)$, which we interpret as the vector potential of the classical external electromagnetic field.

It is straight forward (Eberly 1969) to show that the S-matrix operator corresponding to an arbitrary generalised coherent state is given as

$$\begin{aligned} S_{\psi} = {} & \sum_{n=0}^{\infty} \frac{(-ie)^n}{n!} \int_{VT} d^4x_1 \cdots \int_{VT} d^4x_n \\ & \times \sum_{\{\psi\}} \mathrm{T}[\overline{\psi}(x_1)\hat{A}(x_1)\psi(x_1) \cdots \overline{\psi}(x_n)\hat{A}(x_n)\psi(x_n)] \,, \end{aligned} \tag{4}$$

where the summation $\sum_{\psi}$ is over all possible combinations of substituting the classical vector potential $A^{\mu}_{e}(x)$ for the photon field operator $A^{\mu}(x)$.

For a more realistic description of the focal region than a plane wave, we employ the integral representation* developed by Richards and Wolf (Wolf 1959; Richards and Wolf 1959). This provides the electromagnetic field resulting from

* Such an integral representation has also been used as a basis to estimate the total transition rate for pair production in a focused optical laser field using semi classical Euler–Heisenberg Lagrangian field theoretic methods (Bunkin and Tugov 1970).

photons whose momentum distribution is contained within the cone of directions subtended by the focal point and the aperture of the focusing device. For each such direction the corresponding photon momentum will be of magnitude k_F—the momentum of the incident (unfocused) object region plane wave. Although Wolf's (1959) original derivation exploited some of the approximations contained within geometrical optics, we may apply such a description to the hard X-ray regime because such assumptions are a relic of the optical focusing device assumed—a simple ideal lens. Different methods are used for the focusing of hard X-rays where similar ray tracing techniques are often used to determine the theoretical field distribution of a particular device (Wolter 1952; Chapman *et al.* 1991). In the present context we regard the Richards and Wolf integral representation as *a possible* description containing the essential aspects (inhomogeneities) of a focused field. Whether or not such a description is an accurate one for a given hard X-ray focusing device will not be considered in the present work.

The corresponding generalised coherent state for the Richards and Wolf integral representation is defined via ρ and given by*

$$\rho_{\vec{q}} = f l_0 \frac{\sqrt{\cos\theta_{\vec{q}}}}{\sqrt{2\omega_F}} \sqrt{L}\delta_{|\vec{q}|,\omega_F}\Theta(\theta_{\vec{q}} - \alpha) \,, \tag{5}$$

where f is the focal length and α is the aperture angle of the focusing device, l_0 is the incident electric field of the object region (unfocused) plane wave and L is the side length of the volume V to which the non-laser particles are normalised. Note that α and f are related via $\tan\alpha = r/f$, where r is the radius of the aperture exit. Here spherical polar coordinates are used, where the polar axis is along the optical axis and the azimuthal angle is taken with respect to the direction of the initial electric field (which is perpendicular to the optical axis). Note again that all quantities are expressed in natural units.

The form of equation (5) can best be appreciated by considering $|\rho_{\vec{q}}|^2$ which is equal to the photon number for mode $\vec{q}$. We then have

$$\frac{l_0^2}{2\omega_F} \times f^2 L\cos\theta_{\vec{q}} \times \delta_{|\vec{q}|,\omega_F}\Theta(\theta_{\vec{q}} - \alpha) \,, \tag{6}$$

where the first factor corresponds (in natural) units to the photon number *density* in the object region and the second factor, the adjusted image-space photon normalisation volume determined from the classical geometrical optics intensity law. Here, as in equation (5), the Kronecker-delta and step functions are used to define the allowable modes.

If we choose $A_e^\mu(x)$ (equation 3) to be in the radiation gauge, the temporal part of the polarisation vector is zero and the spatial part is perpendicular to the corresponding laser photon momentum vector. Upon inspection of the vectorial properties determined by Richards and Wolf, the associated spatial polarisation vector in this gauge is given by

$$\vec{\varepsilon}^{\mu}(\vec{q}) = \left(\cos\theta_{\vec{q}} + \sin^2\phi_{\vec{q}}(1-\cos\theta_{\vec{q}}), (\cos\theta_{\vec{q}} - 1)\cos\phi_{\vec{q}}\sin\phi_{\vec{q}}, -\sin\theta_{\vec{q}}\cos\phi_{\vec{q}}\right) \,, \tag{7}$$

* The precise way in which this equation is derived will be detailed in a subsequent publication.

where $\vec{\varepsilon}(\vec{q}) \cdot \vec{q} = 0$ is indeed satisfied.

3. Stimulated Vacuum Pair Production Transition Rate

For stimulated pair production we wish to calculate the transition amplitude

$$\{\langle p^+, r^+| \otimes \langle p^-, r^-|\} S_\psi |0\rangle \,, \tag{8}$$

where $|p^+, r^+\rangle$ ($|p^-, r^-\rangle$) is the non-interacting occupation number state for a positron (electron) with momentum p^+ (p^-) and spin r^+ (r^-), and $|0\rangle$ is the state describing the non-interacting vacuum *external to the laser the field*. The corresponding Feynman diagrams for the expansion of this operator to second order in the electron charge and the laser field are shown in Fig. 1. The normally ordered integral S_ψ operator for the second (lowest) order process is given by

$$S_\psi^{(2)} = ie^2 \int \int_{VT} \mathrm{N}[\overline{\psi}(x_1)\hat{A}_e(x_1)S_F(x_1 - x_2)\hat{A}_e(x_2)\psi(x_2)]d^4x_1 d^4x_2 \,. \tag{9}$$

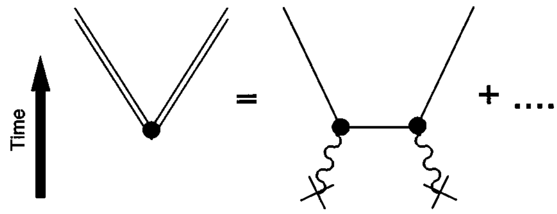

Fig. 1. Feynman diagrams corresponding to the lowest order process contributing to the vacuum pair production process in the presence of an arbitrary external electromagnetic field. Here the photon lines beginning with a cross represent laser photons.

Using the usual finite space–time (VT) Fourier representations of the fermion field operators and propagator (Mandl and Shaw 1988), the pair production amplitude can be written as

$$\{\langle p^+, r^+| \otimes \langle p^-, r^-|\} S_\psi^{(2)} |0\rangle = \overline{\mu}_{r_{\vec{p}^-}}(\vec{p}^-) M(\vec{p}^+, \vec{p}^-) v_{r_{\vec{p}^+}}(\vec{p}^+) \,, \tag{10}$$

where

$$M(\vec{p}^+, \vec{p}^-) = \frac{ie^2 m \delta_{E_{\vec{p}^+} + E_{\vec{p}^-}, 2\omega_F} (VT)^2}{\sqrt{4E_{\vec{p}^+} E_{\vec{p}^-} \omega_F^2 V^4}} \sum_{\vec{q}_1} \rho_{\vec{q}_1} \rho_{\vec{p}^+ + \vec{p}^- - \vec{q}_1}$$
$$\times \, \hat{\varepsilon}(\vec{q}_1) \frac{1}{\hat{p}^- - \hat{q}_1 - m} \hat{\varepsilon}(\vec{p}^+ + \vec{p}^- - \vec{q}_1) \,. \tag{11}$$

Here the hat notation (e.g. $\hat{q}$) represents the Feynman slash vector. Note the energy conserving Kronecker-delta and the remaining laser photon momentum summation which includes all allowable laser momentum contributions to the pair creation process.

The unpolarised finite volume differential transition rate is

$$\Delta\Gamma(\vec{p}^+,\vec{p}^-) = \frac{\sum\limits_{r_{\vec{p}^-},r_{\vec{p}^+}} |\bar{\mu}_{r_{\vec{p}^-}}(\vec{p}^-)M(\vec{p}^+,\vec{p}^-)v_{r_{\vec{p}^+}}(\vec{p}^+)|^2}{T}\frac{V^2\Delta^3\vec{p}^+\Delta^3\vec{p}^-}{(2\pi)^6}\,, \qquad (12)$$

which for equation (11) is proportional to L^4 and thus divergent for $V \to \infty$. This is a consequence of treating the incident laser beam as a plane wave of infinite transverse extent rather than a finite photon flux through the aperture plane. Two factors of L^2 are obtained since equation (12) calculates the pair creation rate arising from two laser photons. This divergence can be corrected for, by replacing each remaining factor of L^2 with the aperture exit area $(\pi f^2 \tan^2\alpha)$. Hence by multiplying equation (12) by $(\pi f^2\tan^2\alpha)^2/L^4$, we now obtain a finite differential transition rate in the limits $V \to \infty$ and $T \to \infty$. In its evaluation, the electron and positron spin summation is replaced by a trace calculation in the usual way.

We wish to calculate the differential transition rate with respect to the direction of the final positron and therefore integrate equation (12) over $\vec{p}^-$ and $|\vec{p}^+|$. This results in a nine-dimensional integral* because the effect of the trace calculation is to mix the 'square' of the laser momentum integration (summation) contained in equation (11). These integrals are determined numerically via an adaptive integration procedure.

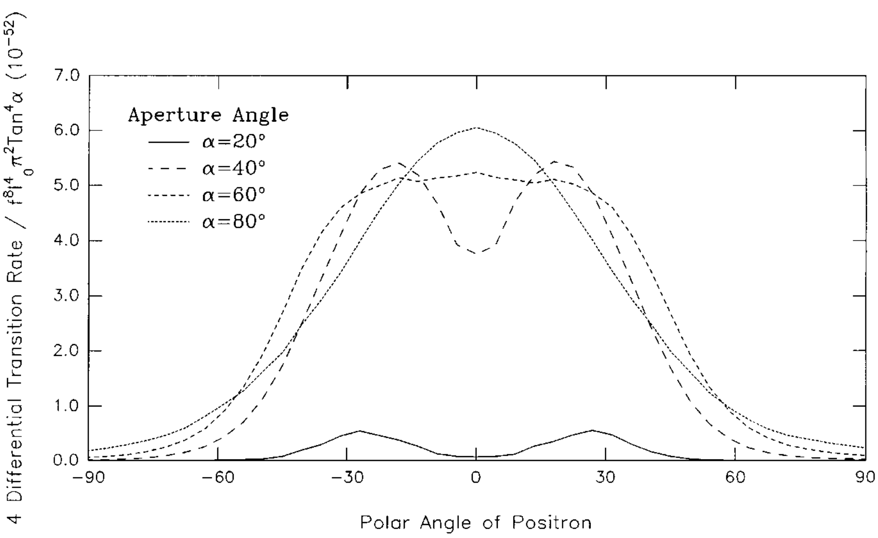

Fig. 2. Focused field differential transition rate for the vacuum pair creation process. The polar angle of the positron ranges between $-90°$ and $90°$, and its azimuthal angle is $0°$. The aperture angle ranges between $20°$ and $80°$ and the focused field laser photon energy is 1 MeV.

* $|\vec{p}^+|$ integration is trivial via the energy conserving delta function.

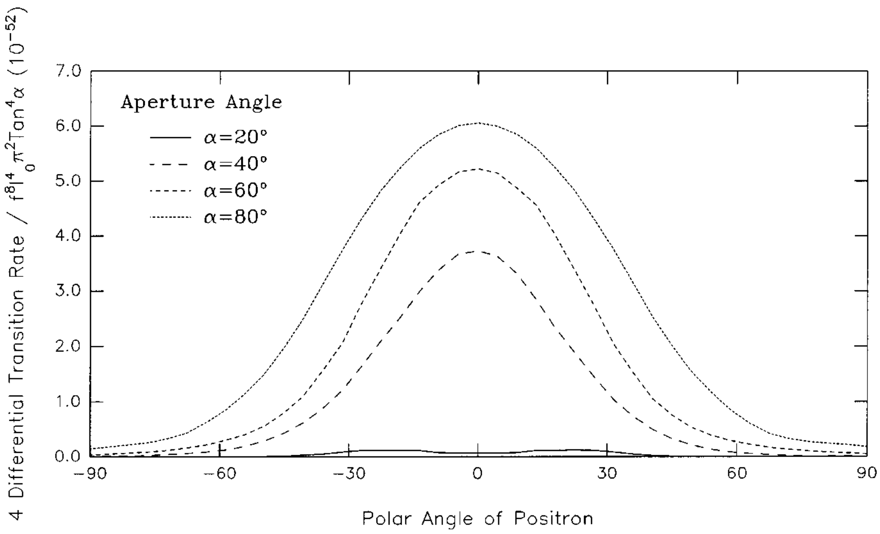

Fig. 3. Focused field differential transition rate for the vacuum pair creation process. The polar angle of the positron ranges between $-90°$ and $90°$, and its azimuthal angle is equal to $90°$. The aperture angle ranges between $20°$ and $80°$ and the focused field laser photon energy is 1 MeV.

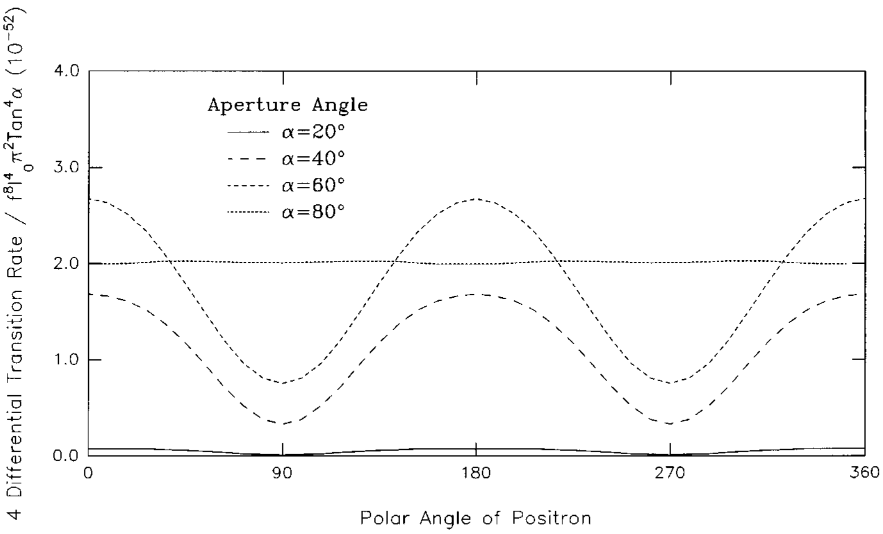

Fig. 4. Focused field differential transition rate for the vacuum pair creation process. The azimuthal angle of the positron ranges between $0°$ and $360°$, and its polar angle is $45°$. The aperture angle ranges between $20°$ and $80°$ and the focused field laser photon energy is 1 MeV.

4. Results

Figs 2 to 4 display the differential transition rate for a range of final scattering directions of the newly created positron for a focused laser field consisting of 1 MeV photons with aperture angles equal to $20°$, $40°$, $60°$ and $80°$. All differential transition rates are in terms of the factor $\frac{1}{4}\pi^2 f^8 l_0^4 \tan^4\alpha$ (in natural units) giving the vertical axis units of electron volts. Again spherical polar coordinates are used with the polar axis along the optical axis and the azimuthal angle taken from the direction of the incident electric field.

Fig. 2 is for an azimuthal angle of 0° (in the plane parallel with the incident electric field) and Fig. 3 is for an azimuthal angle of 90° (in the plane perpendicular to it). For both figures the polar angle continuously ranges between −90° and 90°. For Fig. 4 the polar angle is held constant at 45° and the azimuthal angle is varied between 0° and 360°.

As expected the dominant direction which the positron emerges is along the optical axis. We see that for small aperture angles ($\sim 20°$), a twin peak structure is apparent which is more prominent for the azimuthal angle of 0°. For an azimuthal angle of 90° such a structure is lost for the larger aperture angles (becoming a central peak directed along the optical axis), whereas for an angle of 0° the twin peak structure is maintained up to an aperture angle of nearly 60°, above which, a central peak emerges similar to that for an azimuthal angle of 90°. These observations are also reflected in Fig. 4 where, as a function of the azimuthal angle, an oscillatory differential transition rate arises from the alternating central peak and twin peak structure.

The precise origin of the directional dependence is complicated and a result of internal laser photon momentum integrals over a large trace integrand. The general structure is nevertheless strongly dependent on the angular dependence of the laser photon number density. Inspection of equation (5) reveals that the photon number density $|\rho_{\vec{q}}|^2$ falls off as $\cos\theta_{\vec{q}}$. Consequently the amplitude squared of the process will be roughly dependent on the square of this [see equations (11) and (12)] indicating a peak centred along the optical axis.

The alternating twin peak and central peak structure reflects an asymmetry with respect to the azimuthal angle which can only be due to the incident plane polarised electric field and thus the distribution of laser photon polarisation vectors in the image space region. Since the positron can interact with the laser photon polarisation vectors via its spin, the trace calculation will produce 4-vector products between p^+ and $\varepsilon(\vec{q})$, giving the trace a non-trivial dependence on the cosine of the angle between $\vec{p}^{\,+}$ and $\vec{\varepsilon}(\vec{q})$ [and implicitly between $\vec{p}^{\,-}$ and $\vec{\varepsilon}(\vec{q})$].

For low aperture angles there exists a dominant direction of polarisation in the focal region that would be in the direction of the incident (object region) polarisation vector (along l_0); i.e. the laser photon polarisation vectors will have an average azimuthal angle of 0°. If the final positron has an azimuthal angle of 0° (Fig. 2), its polar angle will be equivalent to the angle the positron direction makes with the dominant polarisation direction. The differential transition rate will therefore be a strong function of the trace integral as the positron's polar angle is varied. This is in addition to the angular dependence incurred from the directional dependence of the laser photon number density. However, if the azimuthal angle is 90° (Fig. 3), there is little variation of the dominant polarisation angle with respect to the positron's polar angle and the angular dependence of the differential transition rate will be primarily dependent on the directional dependence of the laser photon number density and no twin peak structure occurs.

For larger aperture angles, the range of available laser photon momentum directions, and thus laser polarisation vectors, is increased and the above effects are averaged out in the internal laser momentum integrals. This is apparent in the similarities between Figs 2 and 3 for large aperture angles and the almost constant dependence of the differential transition rate as a function of positron azimuthal angle in Fig. 4 for an aperture angle of 80°.

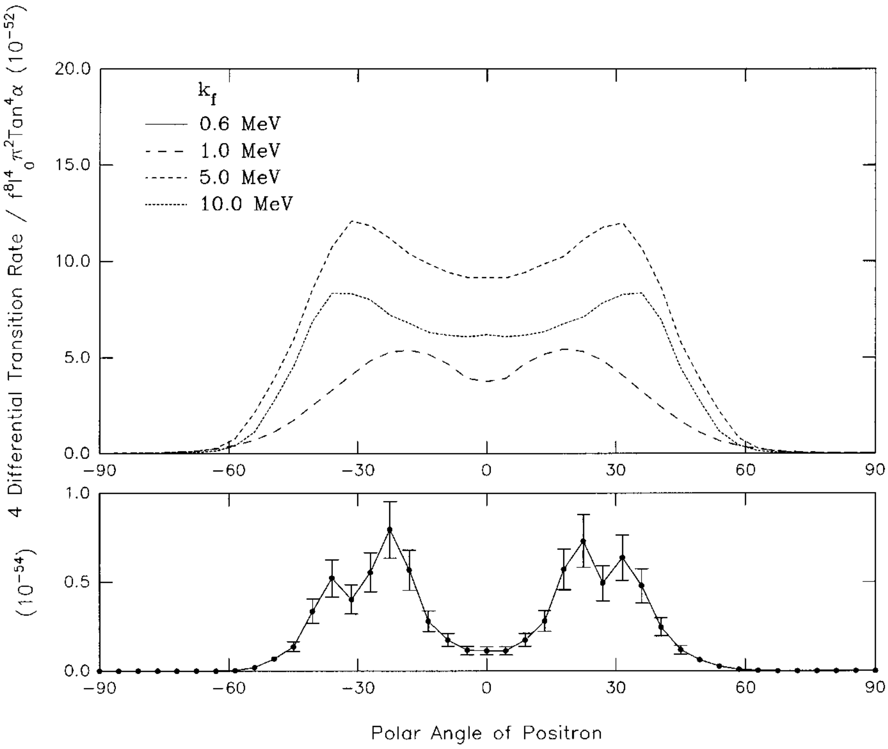

Fig. 5. Focused field differential transition rate for the vacuum pair creation process. The polar angle of the positron ranges between −90° and 90°, and its azimuthal angle is equal to 0°. The aperture angle is equal to 40° and the focused field laser photon energy is 0·6, 1, 5 and 10 MeV. The error bars are derived from the numerical errors associated with the evaluation of the trace integral.

Fig. 5 displays the differential transition rate, with a similar angular range to that of Fig. 2, for the laser photon energies 0·6, 1, 5 and 10 MeV, for an aperture angle of 40°. We see that the rates with 0·6 and 1 MeV laser photons differ by three orders of magnitude whereas, above twice the electron mass, there is not such a great variation. We also see that the 10 MeV rate is less than the rate for 1 and 5 MeV laser photons. This arises because for a given intensity (i.e. a particular object region electric field), the laser photon density decreases as the photon energy increases. We therefore would expect the transition rate to begin to decrease at some stage as the laser energy is increased.

5. Discussion

As it stands, our transition rate is in the natural unit of electron volts. To convert to units of inverse seconds we employ the ratio equality $1\ \mathrm{eV}/\hbar = \mathrm{s}^{-1}/6{\cdot}58\times10^{-16}$

giving the differential transition rate in SI units as $d\Gamma_{\rm SI} = 1\cdot 52 \times 10^{15} d\Gamma_{\rm NU}$. To evaluate our differential transition rate for a particular experimental configuration we use the compact laser synchrotron source (CSS) (Sprangle *et al.* 1992). Such a system produces a coherent source of pulsed hard X-rays in the 30 to 1200 keV range, by the Thompson backscattering of photons originating from a T^3 laser system off a beam of high energy electrons accelerated by an RF linac device. The resulting number of photons emitted is 6×10^9 photons per pulse and with a repetition rate of ~ 1 kHz, the average photon flux becomes 6×10^{12} photons per second. The angular spread of the emerging beam ranges between 2 to 10 mrad. Therefore for the beam to attain a radius of 10 cm it must traverse at least a distance of approximately 20 m. At this distance the photon flux per unit area is $1\cdot 91 \times 10^{14}$ m^{-2} s^{-1} corresponding to a power of $1\cdot 91 \times 10^{20}$ eV m^{-2} s^{-1} for 1 MeV photons. If we choose the focal length of our focusing device to be equal to 10 cm (i.e. an aperture angle of 45°), the parameter fl_0 in natural units is equal to $50\cdot 132$ eV using the conversion equality $\hbar c = 1\cdot 97 \times 10^{-7}$ eV m.

Because the CSS is a pulsed system, the meaningful quantity which can be extracted from our calculation is the probability of the pair creation process occurring per laser pulse. For the CSS, the temporal duration of the pulse is 1 picosecond and to obtain the probability per laser pulse we multiply the transition rate (now in s^{-1}) by 1×10^{-12} s. To obtain the differential transition rate per laser pulse for the pair creation process we thus multiply the vertical axis of Figs 2, 3, 4 and 5 by the factor

$$(1\cdot 52 \times 10^{15}) f^4 \pi^2 \tan^4 \alpha \frac{(fl_0)^4}{4} (1 \times 10^{-12}) = 1\cdot 57 \times 10^{33}\,. \tag{13}$$

From Fig. 3, the central peak has an average height of approximately 4×10^{-52} eV. Hence the differential probability per pulse is approximately $6\cdot 29 \times 10^{-19}$. With a repetition rate of ~ 1 kHz this is increased to $6\cdot 29 \times 10^{-16}$ emerging positrons per second. To gain an order of magnitude estimate of the total probability, we use the data from Figs 3 and 4 for $\alpha = 40°$ to fit a two-dimensional function (in terms of the polar and azimuthal angle of the positron) which is integrated over all directions. This gives a total average number of positrons emitted per second of $3\cdot 21 \times 10^{-14}$. If we were to increase the average photon flux by three orders of magnitude this would become an average of 10^{-8} to 10^{-9} positrons per second—a more amenable (albeit still microscopic) rate to measure.

6. Concluding Remarks

In conclusion, we have presented the quantum electrodynamical differential transition rate for pair creation in a focused hard X-ray laser field which allows an order of magnitude estimate of the stimulated vacuum pair creation rate. This has been made possible by going beyond the plane wave approximation to the focused field and calculating the lowest order contribution with respect to the focused laser field. By extrapolating today's hard X-ray laser and focusing technology to parameter regimes that may be accessible in the near future, we have demonstrated that, in principle, it could be possible to detect the presence of newly created positrons (and indeed electrons) from the centre of a focused laser field.

References

Becker, W. (1991). *Laser and Particle Beams* **9**, 603.
Brezin, E., and Itzykson, C. (1970). *Phys. Rev.* D **2**, 1191.
Bunkin, F. V., and Tugov, I. I. (1970). *Sov. Phys. Doklady* **14**, 678.
Caldi, D. G. (1992). *Phys. Lett.* B **287**, 185.
Chapman, H. N., *et al.* (1991). *Rev. Sci. Instrum.* **62**, 1542.
Derlet, P. M., *et al.* (1995). *Phys. Lett.* A **209**, 154.
Eberly, J. H. (1969). *Progress Optics* **7**, 359.
Glauber, R. J. (1951). *Phys. Rev.* **84**, 395.
Glauber, R. J. (1963). *Phys. Rev.* **130**, 2529.
Jauch, J. M., and Rohlich, F. (1980). 'The Theory of Photons and Electrons', Ch. 14 (Springer: Berlin).
McDonald, K. T., *et al.* (1992). Proc. Workshop on Beam–Beam and Beam–Radiation Interactions—High Intensity and Nonlinear Effects, p. 127 (World Scientific: Singapore).
Mandl, F., and Shaw, G. (1988). 'Quantum Field Theory', Ch. 7 (Wiley: New York).
Nikishov, A. I., and Ritus, V. I. (1967). *Sov. Phys. JETP* **25**, 1135.
Normand, D., *et al.* (1990). *Optics Lett.* **15**, 1400.
Oleinik, V. P. (1967). *Sov. Phys. JETP* **25**, 697.
Oleinik, V. P. (1968). *Sov. Phys. JETP* **26**, 1132.
Richards, B., and Wolf, E. (1959). *Proc. R. Soc. London* A **253**, 358.
Sauteret, C., *et al.* (1991). *Optics Lett.* **16**, 238.
Schwinger, J. (1951). *Phys. Rev.* **82**, 664.
Sprangle, P., *et al.* (1992). *J. Appl. Phys.* **72**, 5032.
Squire, J., *et al.* (1991). *Optics Lett.* **16**, 324.
Volkov, D. M. (1935). *Z. Phys.* **94**, 250.
Wolf, E. (1959). *Proc. R. Soc. London* A **253**, 349.
Wolter, H. (1952). *Ann. Phys. (New York)* **10**, 92; 286.

Manuscript received 25 September 1996, accepted 8 January 1997